Published in final edited form as:
J Chem Theory Comput. 2016 August 09; 12(8): 3482–3490. doi:10.1021/acs.jctc.6b00388.

Toward a general yet effective computational approach for diffusive problems: variable diffusion tensor and DVR solution of the Smoluchowski equation along a general one-dimension coordinate

Andrea Piserchia[*] and **Vincenzo Barone**
Scuola Normale Superiore, piazza dei Cavalieri 7, I-56126 Pisa, Italy

Abstract

A generalization to arbitrary large amplitude motions of a recent approach to the evaluation of diffusion tensors [*J. Comput. Chem.*, **2009**, *30*, 2-13] is presented and implemented in a widely available package for electronic structure computations. A fully black-box tool is obtained, which, starting from the generation of geometric structures along different kinds of paths, proceeds toward the evaluation of an effective diffusion tensor and to the solution of one-dimensional Smoluchowski equations by a robust numerical approach rooted into the discrete variable representation (DVR). Application to a number of case studies shows that the results issuing from our approach are identical to those delivered by previous softwares (in particular DiTe) for rigid scans along a dihedral angle, but can be improved by employing relaxed scans (*i.e.* constrained geometry optimizations) or even more general large amplitude paths. The theoretical and numerical background is robust and general enough to allow quite straightforward extensions in several directions (*e.g.* inclusion of reactive paths, solution of Fokker-Planck or stochastic Liouville equations, multidimensional problems, free-energy rather than electronic-energy driven processes).

1 Introduction

Interpretation of experimental (especially spectroscopic) data in terms of structural and dynamical characteristics of molecular systems of increasing complexity is of paramount interest, but remains often not straightforward. In this connection, the role of computational simulations is constantly increasing in parallel with the improvement of hardware and, especially, of theoretical models and of the corresponding software. In several cases motions of the whole molecular system (*e.g.* global tumbling of the solute in a solvent) and internal degrees of freedom can be defined as diffusive parameters, which, in turn, can be effectively described in terms of an effective tensorial quantity, the diffusion tensor.

Several proposals have been published in recent years, which employ different general assumptions and hydrodynamic models. A comprehensive review of the most interesting approaches has been recently published by Torre and Bloomfield.1 The main limitation of

[*] andrea.piserchia@sns.it; Tel: +39 050 50 9347.

Europe PMC Funders Author Manuscripts

these models is that they can be applied either to rigid molecules (*e.g.* the HYDRONMR software2) or offer a quite limited choice of large amplitude internal motions (essentially torsions like, *e.g.*, in the DiTe approach3). However, chemists are often faced with diffusive problems involving motion along more general paths, which can be parametrized only in terms of a generalized coordinate lacking an overall analytical expression, but rather described only numerically by a non-linear combination of local (curvilinear) coordinates.

A general approach for building such a generalized coordinate involves three main steps. The first one is the generation of an ordered series of geometrical structures visited by the system under study. The simplest way of obtaining these structures involves a rigid or relaxed (*i.e.* constrained optimization of all the other variables) scan along a predefined internal coordinate. More refined strategies range from steepest-descent paths originating from first-order saddle points (the length along this path is the well-known intrinsic reaction coordinate, IRC)4 to principal component analyses (PCA) of molecular dynamics (MD) simulations.5 In the second step, the variation of angular momentum between pairs of successive structures must be minimized, in order to minimize the coupling between the generalized coordinate and the overall rotations of the molecular system. Note that this step leads also to the minimization of the corresponding couplings in the diffusion tensor. Finally, the generalized coordinate is computed as the distance in mass-weighted Cartesian coordinates between successive structures. This choice leads to kinematic computations characterized by a unitary reduced mass. Once the generalized coordinate has been computed, it can be used, for instance, in a quantum mechanical (QM) context to compute vibrationally averaged values of observables solving an effective one-dimensional Schrödinger equations.

Several applications of this approach have been reported for different spectroscopies mostly employing a relaxed scan definition of the generalized coordinate.6–9 Of course, the IRC route has been pioneered by Fukui and further developed by Miller in terms of the so-called reaction path Hamiltonian.4,10,11 Much less work has been performed along these lines in a classical mechanical context, especially in connection with diffusion problems.

This is the main topic of the present work, in which we have implemented in the context of the Gaussian package12 an extension to generalized coordinates of the diffusion tensor approach proposed in previous works.3,13,14 Although the specific applications presented in the following employ rigid or relaxed scans, the implementation permits also the use of IRC or PCA5 paths. The final goal is to build a reliable framework for setting up and solving the one-dimensional Smoluchowski equation along any generalized coordinate, making use of a quite powerful solution method based on the so called Discrete Variable Representation (DVR).15 Once both the main pieces of information (dissipation and energetics) are given and after the diffusive problem solved, some specific quantities (*e.g.* time correlation functions) can be connected to the dynamical quantities of interest (*e.g.* magnetic relaxation times). Furthermore, in some cases, it becomes possible to establish a connection between the continuum diffusive process along a generalized coordinate and the discrete kinetic process between well separated potential energy minima, thus enabling the calculation of rate constants,13–16 which have a close connection with the phenomenological parameters extracted from experimental data.

In our opinion the diffusion tensor approach sketched above can be applied, in addition to the Smoluchowski equation, also in the context of the stochastic Liouville equation (SLE), which is at the heart of the most refined integrated models for the simulation of electronic paramagnetic resonance (EPR) spectra17–22or in connection with the Fokker-Planck equation, which plays a comparable role in the simulation of nuclear magnetic resonance (NMR) spectra.23–25

The paper is organized as follows. The section “Modeling” provides a short description of the approach used to compute the diffusion tensor along a generalized coordinate. The sections “Implementation” and “Case studies” give essential details about the actual numerical implementation of the approach and the main results obtained for a couple of specific cases of chemical interest. Finally, the section “Conclusions” is devoted to some general considerations and most interesting perspectives.

2 Modeling

A molecular system made of N material points (see Fig. 1) is considered, representing the atoms of a molecule without constraints, immersed in a continuous medium with viscosity η. The Cartesian positions $\mathbf{r}_\alpha$ ($\alpha = 1, \dots, N$) of the atoms are referred to a Laboratory Frame (LF) and the associated velocities $\mathbf{v}_\alpha = \dot{\mathbf{r}}_\alpha$ as well. Also a Molecular Frame (MF) is defined and placed on the center of mass of the system, with new atom coordinates $\mathbf{c}_\alpha$. The Cartesian forces acting on the material points are associated to velocities via the $3N \times 3N$ friction matrix $\boldsymbol{\Xi}$

$$\begin{pmatrix} \mathrm{F}_1 \\ \vdots \\ \mathrm{F}_\alpha \\ \vdots \\ \mathrm{F}_N \end{pmatrix} = -\,\Xi \begin{pmatrix} \mathrm{v}_1 \\ \vdots \\ \mathrm{v}_\alpha \\ \vdots \\ \mathrm{v}_N \end{pmatrix} \quad (1)$$

For the constrained system an external coordinate set $[\boldsymbol{\rho}, \boldsymbol{\Omega}, \boldsymbol{q}]$ is defined, where $\boldsymbol{\rho}$ represents the distance of the system center of mass from the LF, $\boldsymbol{\Omega}$ collects the three Euler angles that bring the LF to the MF and $\boldsymbol{q}$ are the $3N - 6$ internal coordinates. Now a subset of the internal coordinates $\boldsymbol{x} : x_1, \dots, x_n$ with $n < 3N - 6$ is selected and the remaining ones, $\boldsymbol{y} : y_1, \dots, y_{3N-6-n}$ are kept frozen; a new set of external coordinates $\mathscr{R} = [\boldsymbol{\rho}, \boldsymbol{\Omega}, \boldsymbol{x}]$ is now considered. Associated to the external coordinates there is the velocity set $\mathscr{V} = [\boldsymbol{v}, \boldsymbol{\omega}, \dot{\boldsymbol{x}}]$, including, the translational velocity, the angular velocity and the internal moments. The total force is composed as well of three contributions $\mathscr{F} = [\boldsymbol{f}, \boldsymbol{\tau}, \boldsymbol{\tau}_x]$, namely, the translational force, the torque and the internal forces. Now, the new relation is

$$\begin{pmatrix} f \\ \tau \\ \tau_x \end{pmatrix} = -\,\xi \begin{pmatrix} v \\ \omega \\ \dot{x} \end{pmatrix} \quad (2)$$

with $\boldsymbol{\xi}$ the (6 + n) × (6 + n) friction matrix for the constrained system.

It can be easily shown14,26 that $\boldsymbol{\mathcal{F}}$ = **A F** and **v** = **B**$\mathcal{V}$, where **A** and **B** are matrices of dimension, (6 + n) × 3N and 3N × (6 + n) respectively that depend only on instantaneous molecular geometry. Also it can be shown that **B** = $\mathbf{A}^{\mathrm{tr}}$ and after some algebra we arrive to

$$\boldsymbol{\xi}=\mathbf{B}^{\mathrm{tr}}\boldsymbol{\Xi}\mathbf{B}=\begin{pmatrix}\boldsymbol{\xi}_{TT} & \boldsymbol{\xi}_{TR} & \boldsymbol{\xi}_{TI}\\ \boldsymbol{\xi}_{RT} & \boldsymbol{\xi}_{RR} & \boldsymbol{\xi}_{RI}\\ \boldsymbol{\xi}_{IT} & \boldsymbol{\xi}_{IR} & \boldsymbol{\xi}_{II}\end{pmatrix} \quad (3)$$

where the subscripts *T, R, I* stand, respectively, for translational, rotational, internal contributions. In order to find the expression for the **B** matrix the Cartesian velocities $\mathbf{v}_{\alpha}$ are expressed with respect to the external coordinates, using simple classical mechanics relations27

$$\mathbf{v}_{\alpha}=\boldsymbol{\upsilon}+\mathbf{E}^{\mathrm{tr}}(\boldsymbol{\Omega})\cdot\left(\boldsymbol{\omega}\times\mathbf{c}_{\alpha}+\sum_{\mu=1}^{n}\frac{\partial\mathbf{c}_{\alpha}}{\partial x_{\mu}}\dot{x}_{\mu}\right) \quad (4)$$

with **E**(**Ω**) the Euler matrix that brings the LF into the MF. Therefore,

$$\begin{pmatrix}\mathbf{v}_1\\ \vdots\\ \mathbf{v}_{\alpha}\\ \vdots\\ \mathbf{v}_N\end{pmatrix}=\begin{pmatrix}\mathbf{1}_3 & -\mathbf{E}^{\mathrm{tr}}(\Omega)\,\mathbf{c}_1^{\times} & \mathbf{E}^{\mathrm{tr}}(\boldsymbol{\Omega})\frac{\partial\mathbf{c}_1}{\partial x_1} & \cdots & \mathbf{E}^{\mathrm{tr}}(\boldsymbol{\Omega})\frac{\partial\mathbf{c}_1}{\partial x_n}\\ \vdots & \vdots & \vdots & & \vdots\\ \mathbf{1}_3 & -\mathbf{E}^{\mathrm{tr}}(\boldsymbol{\Omega})\,\mathbf{c}_{\alpha}^{\times} & \mathbf{E}^{\mathrm{tr}}(\boldsymbol{\Omega})\frac{\partial\mathbf{c}_{\alpha}}{\partial x_1} & \cdots & \mathbf{E}^{\mathrm{tr}}(\boldsymbol{\Omega})\frac{\partial\mathbf{c}_{\alpha}}{\partial x_n}\\ \vdots & \vdots & \vdots & & \vdots\\ \mathbf{1}_3 & -\mathbf{E}^{\mathrm{tr}}(\boldsymbol{\Omega})\,\mathbf{c}_N^{\times} & \mathbf{E}^{\mathrm{tr}}(\boldsymbol{\Omega})\frac{\partial\mathbf{c}_N}{\partial x_1} & \cdots & \mathbf{E}^{\mathrm{tr}}(\boldsymbol{\Omega})\frac{\partial\mathbf{c}_N}{\partial x_n}\end{pmatrix}\begin{pmatrix}\boldsymbol{\upsilon}\\ \boldsymbol{\omega}\\ \dot{\boldsymbol{x}}\end{pmatrix} \quad (5)$$

where $\mathbf{c}_{\alpha}^{\times}$ is the 3 × 3 matrix with elements $\left(\mathbf{c}_{\alpha}^{\times}\right)_{mn}=\sum\varepsilon_{\mathrm{mln}}(\mathbf{c}_{\alpha})_l$ and where $\boldsymbol{\varepsilon}_{mln}$ is the Levi-Civita symbol. It can be readily noticed that **B** is dependent only on the instantaneous geometry and, in principle, knowledge of the derivatives $\frac{\partial\mathbf{c}}{\partial x}$ is required. In the case one wants to deal just with natural internal coordinates, as dihedrals,3 bond angles and/or bond lengths, analytical expressions28 for the derivatives $\frac{\partial\mathbf{c}}{\partial x}$ are well known.

In our treatment the subset ***x*** is reduced to a single generalized coordinate, hereafter called *s*, found by one of the methods sketched in the Introduction. Equation (5) still holds; the derivatives will be now $\frac{\partial\mathbf{c}}{\partial s}$

Once **B** is constructed, the remaining task is to model the unconstrained friction tensor **Ξ**. The simplest model is that of independent beads, *i.e.*

$$\boldsymbol{\Xi}=\Xi_0\mathbf{1}_N \quad (6)$$

with $\Xi_0 = CR_e\,\eta\,\pi$, R_e being the hydrodynamical radius and $C = 4, 6$ the slip or stick, respectively, boundary condition coefficient. The constrained friction tensor is so

$$\boldsymbol{\xi}=\Xi_0\mathbf{B}^{\mathrm{tr}}\mathbf{B} \quad (7)$$

and the requested diffusion tensor is easily calculated using Einstein relation

$$\mathbf{D}=k_BT\boldsymbol{\xi}^{-1}=\begin{pmatrix}\mathbf{D}_{TT} & \mathbf{D}_{TR} & \mathbf{D}_{TG}\\ \mathbf{D}_{RT} & \mathbf{D}_{RR} & \mathbf{D}_{RG}\\ \mathbf{D}_{GT} & \mathbf{D}_{GR} & \mathbf{D}_{GG}\end{pmatrix} \quad (8)$$

where G now stand for generalized. Since we are dealing with just one generalized coordinate, $\mathbf{D}_{GG}$ is a scalar function of s, and hereafter we shall name it simply $D_{GG}(s)$. More sophisticated models can be chosen in order to take into account the effects of hydrodynamic interactions among the beads, using for example the Oseen29,30 or the Rotne-Prager31 model. When evaluating the friction exerted by the medium over a generic bead, these models account for the perturbative effect of the other particle motion over the fluid velocity field. Here, we adopt the Rotne-Prager model since it has the advantage to always provide positive-definite diffusion tensors. Considering two generic atoms α, β the 3 × 3 blocks of the unconstrained diffusion tensor (here called $\boldsymbol{\Delta}$) are then given by

$$\begin{cases}\boldsymbol{\Delta}_{\alpha\alpha}=\frac{k_BT}{\Xi_0}\mathbf{1}_3 & \\ \boldsymbol{\Delta}_{\alpha\beta}=\frac{k_BT}{8\pi\eta r_{\alpha\beta}}\left[\left(1+\frac{2R_e^2}{3r_{\alpha\beta}^2}\right)\mathbf{1}_3+\left(1-\frac{2R_e^2}{r_{\alpha\beta}^2}\right)\frac{\mathbf{r}_{\alpha\beta}\otimes\mathbf{r}_{\alpha\beta}}{r_{\alpha\beta}^2}\right] & \text{if } r_{\alpha\beta}\geq 2R_e\\ \boldsymbol{\Delta}_{\alpha\beta}=\frac{k_BT}{8\pi\eta r_{\alpha\beta}}\left[\frac{r_{\alpha\beta}}{2R_e}\left(\frac{8}{3}-\frac{3r_{\alpha\beta}}{4R_e}\right)\mathbf{1}_3+\frac{\mathbf{r}_{\alpha\beta}\otimes\mathbf{r}_{\alpha\beta}}{8R_e^2}\right] & \text{if } r_{\alpha\beta}\leq 2R_e\end{cases} \quad (9)$$

where $\mathbf{r}_{\alpha\beta} = \mathbf{r}_\alpha - \mathbf{r}_\beta$, $r_{\alpha\beta} = |\mathbf{r}_{\alpha\beta}|$ and ⊗ the dyadic product. From eqn (7) using again Einstein relation (eqn (8)), **D** is easily found as

$$\mathbf{D}=\left(\mathbf{B}^{\mathrm{tr}}\boldsymbol{\Delta}^{-1}\mathbf{B}\right)^{-1} \quad (10)$$

3 Implementation

Here we just provide a short overview about the implementation. In a separate code embedded in the framework of the Gaussian package we have merged the computation of the potential (or free, *vide infra*) energy along the generalized coordinate with the calculation of the diffusion tensor along the same path. In particular during the scan along the internal coordinate, the molecular geometry can be optimized or not (relaxed and non-

relaxed scan). In both cases at each step of the scan, the generalized coordinate s is calculated and the new Cartesian coordinates referred to the MF are given. The MF is chosen at the initial geometry to be fixed on the molecule center of mass and in Eckart orientation; all the following coordinates **c** are referred to this MF; in the present version of the code the derivatives $\frac{\partial \mathbf{c}}{\partial s}$ are calculated numerically, although implementation of analytical derivatives is under way. Several checks have been anyways performed to verify the stability of the numerical approach.

After the boundary conditions are chosen, the only free-parameter is the hydrodynamic radius of the beads R_e. Following ref3 we chose an effective sphere radius as the weighted arithmetic mean

$$R_e = \frac{\sum_X n_X R_X}{\sum_X n_X} \quad (11)$$

where n_X is the number of atoms of type X and R_X is the associated van der Waals (vdW) radius (we use the UFF set of vdW radii32). From this computation and the whole diffusion tensor calculation we only take into account non-hydrogen atoms, since the hydrogen ones are negligible from the consideration of exposed surface “wetted” by the solvent and typically they end up only with numerically spurious contributions.

4 Case-study calculations

In this section we apply the method sketched above in the Modeling section to some case-study molecules. Our goal is to determine $D_{GG}(s)$ from the integrated calculation of the potential scan along the generalized coordinate with the calculation of the diffusion tensor along the same path. In some cases we shall use these two pieces of information to set up and solve a one-dimensional Smoluchowski equation for the generalized coordinate treated as a diffusive one and making use of the novel DVR solving approach.15 The interested reader can find all the details about the DVR implementation in that reference; here we just briefly recall the one-dimensional Smoluchowski equation that reads33–35

$$\frac{\partial}{\partial t} p(x,t) = -\Gamma p(x,t) \quad (12)$$

where $p(x, t)$ is the probability density of finding a value of x at time t, with stationary limit $\lim_{t\to+\infty} p(x,t) = p_{eq}(x)$; in our case x could be the generalized coordinate s or the internal coordinate scanned with DiTe. Γ is the diffusion operator

$$\Gamma = -\frac{\partial}{\partial x} D(x)\, p_{eq}(x)\, \frac{\partial}{\partial x} p_{eq}^{-1}(x) \quad (13)$$

with $D(x)$ a space-dependent diffusion coefficient. In this case

$$p_{eq}(x) = \frac{e^{-\beta V(x)}}{Z} \quad (14)$$

is the canonical (Boltzmann) distribution, for the potential $V(x)$; with $\beta = 1/k_B T$ the Boltzmann factor and $Z = \int dx e^{-\beta V(x)}$ the partition function. Technically, the potential $V(x)$ has the meaning of an Helmholtz free energy at temperature T (in other words a "mean field potential"). Upon representing the symmetrized diffusion operator

$$\tilde{\Gamma} = p_{eq}^{-1/2}(x)\,\Gamma\, p_{eq}^{1/2}(x) \quad (15)$$

in the DVR basis one solves the equation by diagonalization of the same. The eigenvalues λ_i associated to the diffusion operator are all real and positive (since $\tilde{\Gamma}$ is Hermitian and $D(x)$ is a positive function) and they are characterized by the presence of a unique null eigenvalue $\lambda_0 = 0$ associated to $p_{eq}^{-1/2}(x)$ eigenfunction. In the case of diffusive dynamics under the influence of a potential $V(x)$ that presents sufficiently deep wells separated by an energy gap, we can associate to small λ_i values "jump" processes between wells (*i.e.* slow activated processes where it is required to overpass the energy gap); high λ_i values can be associated, instead, to fluctuation processes inside the wells (fast processes).

We shall examine three test cases of chemical interest in order to illustrate the applicability of the method, starting from the internal rotation around the central C-C bond of *n*-butane and we shall compare our results with those delivered by the DiTe software3 showing the reliability of the novel approach. Next, we investigate the inversion motion (envelope twist) of cyclopentene that couldn't be treated with the previous softwares and finally the internal rotation of 3-chloro-2-(chloromethyl)toluene and 2,2'-bifuran. The hydrodynamic boundary constant has been always set equal to $C = 6$, (stick boundary conditions). Since the examined potential and diffusion profiles along s will result periodic, in Appendix A we provide the matrix elements of the diffusion operator expressed in the DVR basis with periodic boundary conditions for a generic range.

n-butane

The generalized coordinate s is calculated along the internal rotation of the central C-C bond θ, starting from the optimized geometry of *n*-butane, and performing both a non-relaxed and a relaxed scan of 100 steps in the range $0° < \theta < 360°$; where $\theta = 0°$ corresponds to the eclipsed conformation (see Fig. 2, panel a). Initially we have performed a non-relaxed scan that is useful in order to compare our results with DiTe ones for the same system. In fact, we can retrieve $D_{II}(\theta)$ (quantity calculated by DiTe) from the knowledge of $D_{GG}(s)$ and of the variations of s with θ, *i.e.* $\frac{ds}{d\theta}$, and this can be done inside our program, again carried out numerically. As it can be seen in panel a of Fig. 3 the two profiles are identical, confirming

the consistency of our approach and the linear variation of s with respect to θ (panel b), as expected from a non-relaxed scan.

Then we have performed a relaxed scan for the same system at the B2PLYP level36,37 using the aug-cc-pVTZ basis,38 adding dispersion corrections by the D3 empirical model39 and including bulk solvent effects of *n*-butane by the conductor version of the polarizable continuum model (C-PCM).40 Note that the energy issuing from this treatment has the status of a free energy41 and the only significant approximation (which can be lifted if needed) is to consider constant the frequencies of small amplitude motions perpendicular to the large amplitude path. The calculated energetics $V(s)$ and diffusion $D_{GG}(s)$ profiles are shown in Fig. 4. We want to stress that there is no direct link between these two quantities. As stated before, they are essential ingredients to set up and solve the Smoluchowski equation for the generalized coordinate treated as a stationary diffusive process. Similarly to what we have done in ref.15 and in the past works of Moro and Nordio, 16,42 we use the two first lowest and non zero eigenvalues and the equilibrium populations in order to calculate the kinetic constants for the transitions between the three stable conformations (eqn (27) in Appendix B). These conformations can be identified with the three wells (marked with an asterisk in panel a of Fig. 4) separated by a sufficiently high energy gap and they geometrically correspond to the two equivalent *gauche* and the *trans* conformation (from now on respectively abbreviated as $g_{\pm}$ and t). Edberg and coworkers43 have calculated the kinetic constant $k_{t\rightarrow g\pm} = 1.9 \times 10^{10}\ s^{-1}$ and $k_{g\pm\rightarrow t} = 2.9 \times 10^{10}\ s^{-1}$ performing a nonequilibrium molecular dynamics simulation of bulk *n*-butane at $T = 292$ K. At the same temperature and using the viscosity of the medium as the one of *n*-butane44 we obtain $k_{t\rightarrow g\pm} = 3.75 \times 10^{9}\ s^{-1}$ and $k_{g\pm\rightarrow t} = 1.17 \times 10^{10}\ s^{-1}$, while assuming the same potential in the [0°, 360°] range but using $D_{II}(\theta)$ calculated from DiTe we obtain $k_{t\rightarrow g\pm} = 3.41 \times 10^{10}\ s^{-1}$ and $k_{g\pm\rightarrow t} = 1.07 \times 10^{10}\ s^{-1}$. The kinetic constants calculated with our method and with Dite are very similar, confirming the reliability of our approach and showing that the relaxation effects of a small molecule like *n*-butane are quite irrelevant. With respect to the values reported in the work of Edberg and coworkers, our $k_{t\rightarrow g\pm}$ in both cases are one order of magnitude smaller, while $k_{g\pm\rightarrow t}$ are very close. We believe that this difference is mainly due to the fact that in our kinetic model we are not accounting for the solvent fluctuations around the molecule, in other words, we are considering the surrounding solvent molecules as if they are at equilibrium.

cyclopentene

The generalized coordinate s is calculated along the envelope movement regulated by a properly defined bending angle φ (see Fig. 2, panel b), performing a relaxed scan of 100 steps in the range $-60° < \varphi < 60°$ where $\varphi = 0°$ correspond to the situation in which the envelope is completely opened (the energy minimum). We want to stress that this kind of computation was unfeasible using previous softwares like HYDRONMR and/or DiTe. The relaxed scan for the same system is performed at the B3LYP level45 adding the D3 dispersion corrections and 6-31++G** basis including bulk solvent effects of carbon tetrachloride by the C-PCM. The potential and $D_{GG}(s)$ are shown in Fig. 5 and, as expected, it can be seen that $V(s)$ is just a parabola inside which the system oscillates around the minimum along s. This is also confirmed after solving the Smoluchowski equation where

there is no neat separation (in terms of orders of magnitude) between the eigenvalues, and consequently they can only be associated to fast processes of fluctuations inside the well.

3-chloro-2-(chloromethyl)toluene and 2,2'-bifuran

The generalized coordinate s is calculated along the internal rotation of 3-chloro-2-(chloromethyl)toluene C-C bond and the central one in 2,2'-bifuran (see Fig. 6), performing a relaxed scan of 100 steps in the range $0° < \omega < 360°$ and $-90° < \psi < 270°$ for 3-chloro-2-(chloromethyl)toluene and 2,2'-bifuran molecules respectively. The relaxed scan for both systems is conducted at B3LYP level adding the D3 dispersion corrections and 6-31++G** basis including bulk solvent effects of carbon tetrachloride by the C-PCM. The potential and the generalized part of the diffusion tensor $D_{GG}(s)$ are shown in Fig. 7 and Fig. 8, as it can be seen they are both bistable with equivalent and nonequivalent minima respectively. Again, it is not possible to make direct inferences between the potential and diffusion profiles. We use them both to set up and solve the Smoluchowski equation for the generalized coordinate treated as a stationary diffusive process and, as in the *n*-butane case, we calculate the kinetic constant for the transitions between the wells. Since this time the number of possible jumps is reduced (the forward and backward jump between the two wells), the kinetic model is different than for the *n*-butane case and this is also the case for the expression that links the eigenvalues to the kinetic constants, k_f and k_b respectively (see eqns (28,29) in Appendix B). At room temperature $T = 298.15$ K and using the viscosity of the medium as the one of carbon tetrachloride44 we obtain $k_f = k_b = 3.18 \times 10^6\ s^{-1}$ for the first molecule and $k_f = 4.30 \times 10^7\ s^{-1}$, $k_b = 2.67 \times 10^8\ s^{-1}$ for the second one. As expected, the huge barrier for 3-chloro-2-(chloromethyl)toluene gives the smallest kinetic constant, while for 2,2'-bifuran, considering that the backward jump faces an energy barrier similar to the ones of *n*-butane jumps, the lower magnitude of diffusion gives globally lower kinetic constants.

5 Conclusions

The main aim of this work is to propose and implement an effective approach for computing diffusion tensors depending on a generalized large amplitude coordinate. The proposed approach is obtained by the integration of previous proposals for diffusive processes (mainly the HYDRONMR and DiTe approaches) with the intrinsic reaction coordinate and reaction path Hamiltonian descriptions of general large amplitude motions. Numerical solutions based on a general implementation of the so called discrete variable representation (DVR) lead to a very effective way of solving one-dimensional Smoluchowski equations for the description of general one-dimensional diffusive processes. The analysis of some case studies involving medium-size molecular systems shows that the new implementation fully agrees with the DiTe results for non relaxed scans, whereas it allows to improve the agreement with experimental results due to its ability of including full relaxation along directions perpendicular to the generalized large amplitude coordinate.

A number of extensions of the approach is possible and already under way in our laboratory. The first step is the solution of systems of coupled Smoluchowski equations including reactive terms,46–51 of particular interest for the study of time resolved fluorescence

Europe PMC Funders Author Manuscripts

experiments or, more generally, of photochemical processes. In parallel, methods for solving stochastic Liouville or Fokker-Planck33 equations can be implemented along the same lines and can be of remarkable interest for instance in connection with magnetic (EPR and NMR) spectroscopies.

A more ambitious target is the extension of the approach to more than one internal generalized coordinate. Work along these lines has already been performed in the quantum mechanical community, leading to the so-called reaction surface Hamiltonian, in which all the remaining internal coordinates are optimized at selected values of two or three large amplitude coordinates.52,53 An alternative is to perform a principal component analysis of a trajectory obtained from *e.g.* molecular dynamics and to select a reduced number of eigenvectors of the covariance matrix (the so-called essential dynamics) as large amplitude coordinates.5 The theoretical machinery for all these approaches is well known and the corresponding stochastic equations can be solved by multidimensional extensions of the DVR approach, which are also well known in the quantum mechanical community.54,55

The numerical stability of the approach is an additional issue. Here, replacement of numerical derivatives by their analytical counterparts is already under way along the same lines one of us has recently followed in connection with vibronic contributions to electronic spectra.56,57 On the other hand, numerical issues connected with the DVR solution have been investigated in detail for one-dimensional problems15 and, in different contexts, also for many-dimensional problems.54,55

A final issue concerns the use of electronic energies in place of (the correct) free energies. From the one side, free-energies can be obtained by computing harmonic frequencies at different values of the large amplitude coordinate for all the remaining orthogonal (small amplitude) motions and employing well known statistical thermodynamics equations. Even leading anharmonicities can be included for those transverse motions by means of *e.g.* second order vibrational perturbation theory (VPT2).9,37,58,59 From another side true dynamical techniques like *e.g.* the so called dynamic reaction coordinate60 or metadynamics61 can be employed to obtain free energies as a function of the large amplitude generalized coordinate.

In conclusion we think that, also pending the further development sketched above, we already have a tour disposal a quite powerful machinery allowing to complement experimental studies for a number of problems of current fundamental and applicative interest.

Supplementary Material

Refer to Web version on PubMed Central for supplementary material.

Acknowledgments

The authors are very grateful to Antonino Polimeno from the University of Padova for useful and fruitful discussions. The research leading to these results has received funding from the European Research Council under the European Union’s Seventh Framework Programme (FP/2007-2013) / ERC Grant Agreement n. [320951].

References

[1]. De La Torre JG, Bloomfield VA. Q Rev Biophys. 1981; 14:81–139. [PubMed: 7025081]

[2]. De La Torre JG, Huertas ML, Carrasco B. J Magn Reson B. 2000; 147:138–146.

[3]. Barone V, Zerbetto M, Polimeno A. J Comput Chem. 2009; 30:2–13. [PubMed: 18496840]

[4]. Fukui K. J Phys Chem. 1970; 74:4161–4163.

[5]. Amadei A, Linssen ABM, Berendsen HJC. Proteins: Struct, Funct, Bioinf. 1993; 17:412–425.

[6]. Barone V. J Chem Phys. 1994; 101:10666–10676.

[7]. Rega N, Cossi M, Barone V. J Am Chem Soc. 1997; 119:12962–12967.

[8]. Improta R, Barone V. Chem Rev. 2004; 104:1231–1254. [PubMed: 15008622]

[9]. Skouteris D, Calderini D, Barone V. J Chem Theory Comput. 2016; 12:1011–1018. [PubMed: 26765363]

[10]. Fukui K. Acc Chem Res. 1981; 14:363–368.

[11]. Miller WH, Handy NC, Adams JE. J Chem Phys. 1980; 72:99–112.

[12]. Frisch, MJ., et al. Gaussian Development Version, Revision I.03. Gaussian, Inc.; Wallingford, CT; 2015.

[13]. Ferrarini A, Moro G, Nordio PL. Mol Phys. 1988; 63:225–247.

[14]. Nigro B, Di Stefano D, Rassu A, Moro GJ. J Chem Phys. 2004; 121:4364–4376. [PubMed: 15332988]

[15]. Piserchia A, Barone V. Phys Chem Chem Phys. 2015; 17:17362–17374. [PubMed: 26078048]

[16]. Moro G, Nordio PL. Mol Phys. 1986; 57:947–955.

[17]. Barone V, Brustolon M, Cimino P, Polimeno A, Zerbetto M, Zoleo A. J Am Chem Soc. 2006; 128:15865–15873. [PubMed: 17147399]

[18]. Carlotto S, Cimino P, Zerbetto M, Franco L, Corvaja C, Crisma M, Formaggio F, Toniolo C, Polimeno A, Barone V. J Am Chem Soc. 2007; 129:11248–11258. [PubMed: 17705490]

[19]. Zerbetto M, Carlotto S, Polimeno A, Corvaja C, Franco L, Toniolo C, Formaggio F, Barone V, P C. J Phys Chem B. 2007; 111:2668–2674. [PubMed: 17311450]

[20]. Zerbetto M, Polimeno A, Cimino P, Barone V. J Chem Phys. 2008; 128:024501. [PubMed: 18205453]

[21]. Zerbetto M, Polimeno A, Barone V. Comput Phys Commun. 2009; 180:2680–2697.

[22]. Zerbetto M, Licari D, Barone V, Polimeno A. Mol Phys. 2013; 111:2746–2756.

[23]. Zerbetto M, Kotsyubynskyy D, Kowalewski J, Widmalm G, Polimeno A. J Phys Chem B. 2012; 116:13159–13171. [PubMed: 23057513]

[24]. Kotsyubynskyy D, Zerbetto M, Soltesova M, Engström O, Pendrill R, Kowalewski J, Widmalm G, Polimeno A. J Phys Chem B. 2012; 116:14541–14555. [PubMed: 23185964]

[25]. Piserchia A, Zerbetto M, Salvia M, Salassa G, Gabrielli L, Mancin F, Rastrelli F, Frezzato D. J Phys Chem C. 2015; 119:20100–20110.

[26]. Moro G. Chem Phys. 1987; 118:181–197.

[27]. Goldstein, H., Poole, CP., Safko, JL. Classical Mechanics. Addison Wesley; Boston: 2002.

[28]. Thompson HB. J Chem Phys. 1967; 47:3407–3410.

[29]. Kirkwood JG, Riseman J. J Chem Phys. 1948; 16:565–573.

[30]. Yamakawa H. J Chem Phys. 1970; 53:436–443.

[31]. Rotne J, Prager S. J Chem Phys. 1969; 50:4831–4837.

[32]. Rappe AK, Casewit CJ, Colwell KS, Goddard WA III, Skiff WM. J Am Chem Soc. 1992; 114:10024–10035.

[33]. Gardiner, CW. Handbook of Stochastic Methods: For Physics, Chemistry and the Natural Sciences; Springer series in synergetics. Springer-Verlag; Berlin Heidelberg, Germany: 1985.

[34]. Zwanzig, R. Nonequilibrium Statistical Mechanics. Oxford University Press; New York: 2001.

[35]. Van Kampen, NG. Stochastic Processes in Physics and Chemistry; North-Holland Personal Library. Elsevier Science; Oxford, UK: 2011.

[36]. Grimme S. J Chem Phys. 2006; 124:034108. [PubMed: 16438568]

[37]. Biczysko M, Panek P, Scalmani G, Bloino J, Barone V. J Chem Theory Comput. 2010; 6:2115–2125. [PubMed: 26615939]
[38]. Kendall RA, Dunning TH, Harrison RJ. J Chem Phys. 1992; 96:6796–6806.
[39]. Grimme S, Antony J, Ehrlich S, Krieg H. J Chem Phys. 2010; 132:154104. [PubMed: 20423165]
[40]. Cossi M, Rega N, Scalmani G, Barone V. J Comput Chem. 2003; 24:669–681. [PubMed: 12666158]
[41]. Tomasi J, Mennucci B, Cammi R. Chem Rev. 2005; 105:2999–3094. [PubMed: 16092826]
[42]. Moro G, Nordio PL. Mol Phys. 1985; 56:255–269.
[43]. Edberg R, Evans DJ, Morriss GP. J Chem Phys. 1987; 87:5700–5708.
[44]. Yaws, CL. Transport Properties of Chemicals and Hydrocarbons. Elsevier Science; Oxford, UK: 2014.
[45]. Becke AD. J Chem Phys. 1993; 98:5648–5652.
[46]. Agmon N, Hopfield JJ. J Chem Phys. 1983; 78:6947–6959.
[47]. Pines E, Huppert D, Agmon N. J Chem Phys. 1988; 88:5620–5630.
[48]. Krissinel' EB, Agmon N. J Comput Chem. 1996; 17:1085–1098.
[49]. Gepshtein R, Huppert D, Agmon N. J Phys Chem B. 2006; 110:4434–4442. [PubMed: 16509746]
[50]. Erez Y, Liu Y, Amdursky N, Huppert D. J Phys Chem A. 2011; 115:8479–8487. [PubMed: 21711024]
[51]. Pedone A, Gambuzzi E, Barone V, Bonacchi S, Genovese D, Rampazzo E, Prodi L, Montalti M. Phys Chem Chem Phys. 2013; 15:12360–12372. [PubMed: 23783271]
[52]. Carrington T, Miller WH. J Chem Phys. 1984; 81:3942–3950.
[53]. Tew DP, Handy NC, Carter S. J Chem Phys. 2006; 125:084313i. [PubMed: 16965018]
[54]. Dawes R, Carrington T. J Chem Phys. 2004; 121:726–736. [PubMed: 15260599]
[55]. Degani I, Tannor DJ. J Phys Chem A. 2006; 110:5395–5410. [PubMed: 16623468]
[56]. Baiardi A, Bloino J, Barone V. J Chem Theory Comput. 2015; 11:3267–3280. [PubMed: 26575763]
[57]. Baiardi A, Bloino J, Barone V. J Chem Phys. 2016; 144:084114. [PubMed: 26931688]
[58]. Barone V. J Chem Phys. 2004; 120:3059–3065. [PubMed: 15268458]
[59]. Barone V, Biczysko M, Bloino J. Phys Chem Chem Phys. 2014; 16:1759–1787. [PubMed: 24346191]
[60]. Maluendes SA, Dupuis M. J Chem Phys. 1990; 93:5902–5911.
[61]. Laio A, Parrinello M. Proc Natl Acad Sci USA. 2002; 99:12562–12566. [PubMed: 12271136]
[62]. Colbert DT, Miller WH. J Chem Phys. 1992; 96:1982–1991.

Europe PMC Funders Author Manuscripts

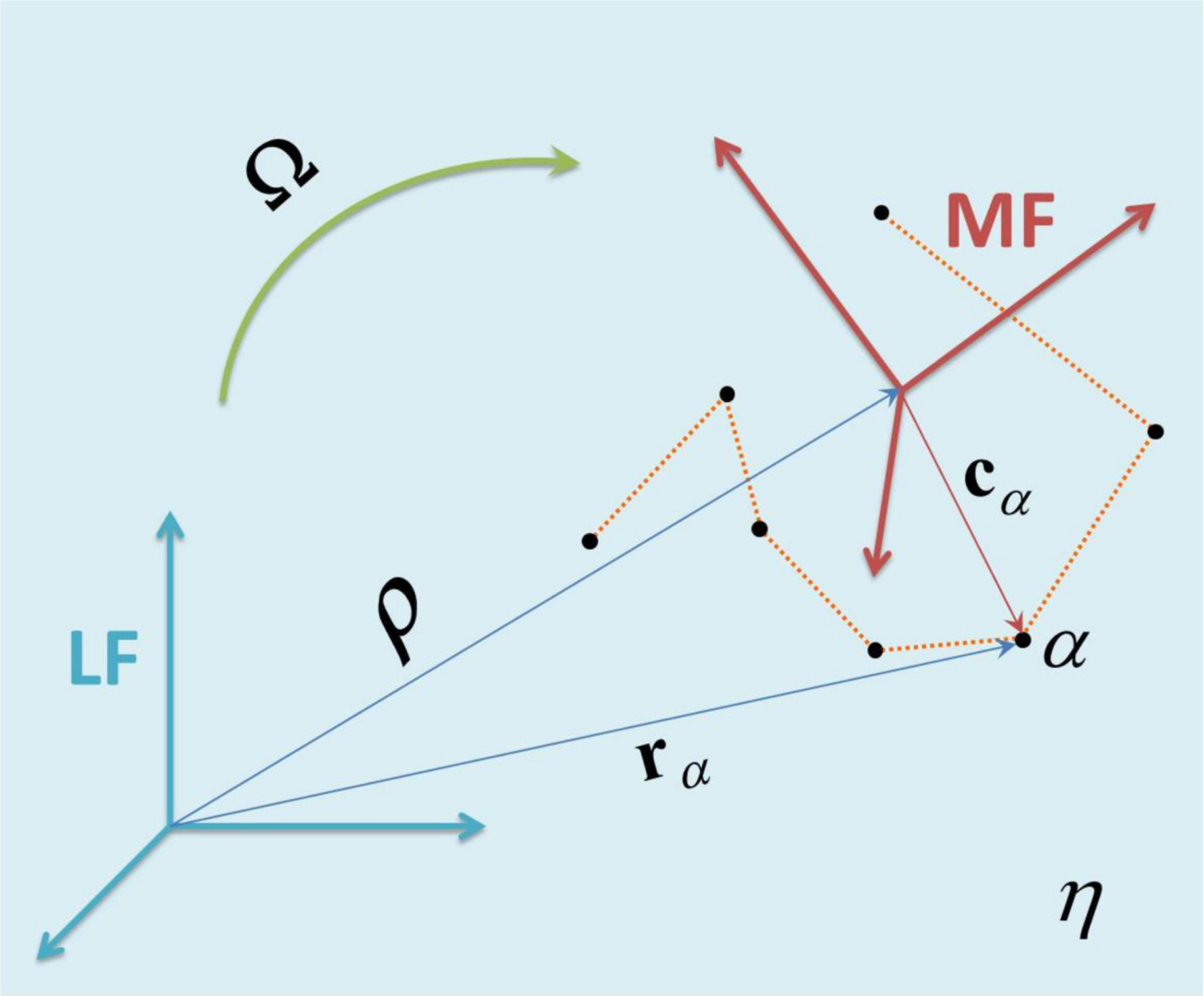

Figure 1.

Sketch of an (un)constrained molecular system and physical quantities involved in the model construction. The dashed orange lines highlight the constraints, while the light blue background indicates the solvent.

Europe PMC Funders Author Manuscripts

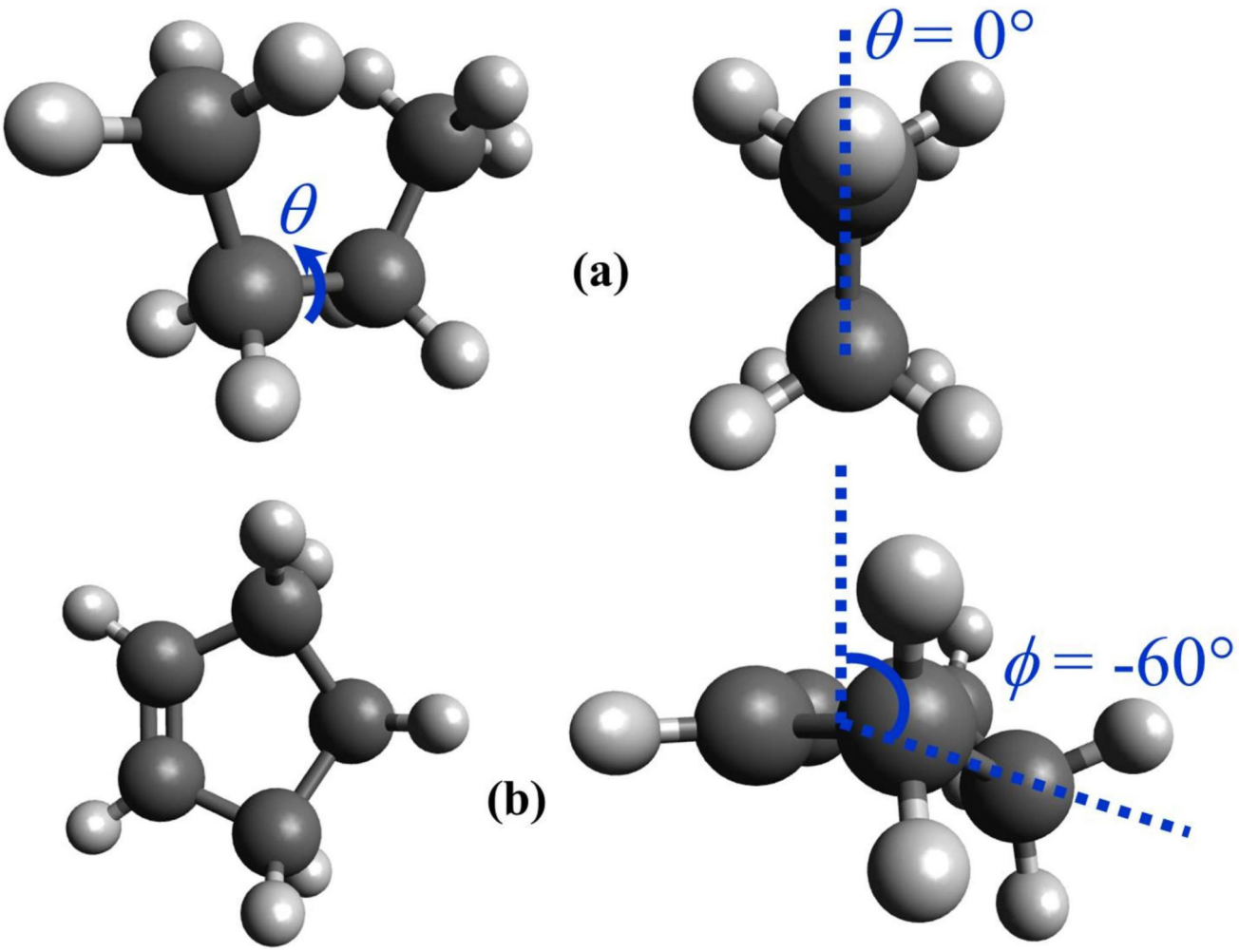

Figure 2.

Sketch of *n*-butane (panel a) and cyclopentene (panel b) starting conformations for the scans along the highlighted internal coordinate.

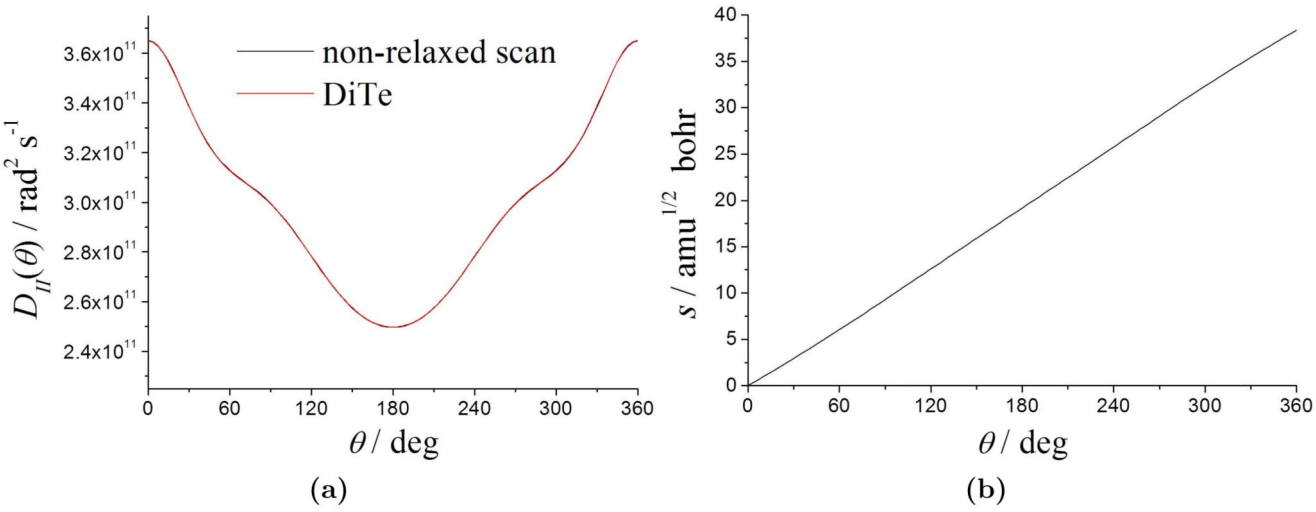

Figure 3.

Panel a; calculated internal component of the diffusion tensor of *n*-butane from the non-relaxed scan (black line) and from DiTe (red line) at $T = 292$ K; the two curves are coincident. Panel b; variation of the generalized coordinate s with respect to the internal rotation θ.

Europe PMC Funders Author Manuscripts

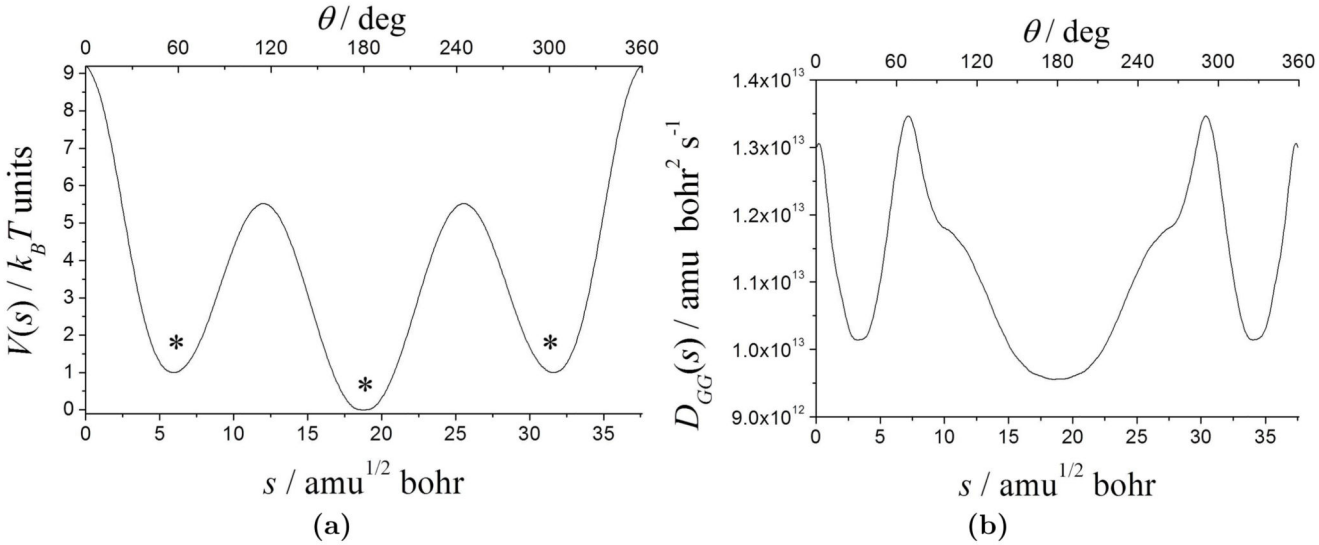

Figure 4.

Calculated potential energy of *n*-butane from the relaxed scan (panel a) and diffusion along the generalized coordinate (panel b). The asterisks on the potential wells highlight the stable conformations. The upper axis shows the corresponding internal coordinate upon which the scan is performed. (T = 292 K)

Europe PMC Funders Author Manuscripts

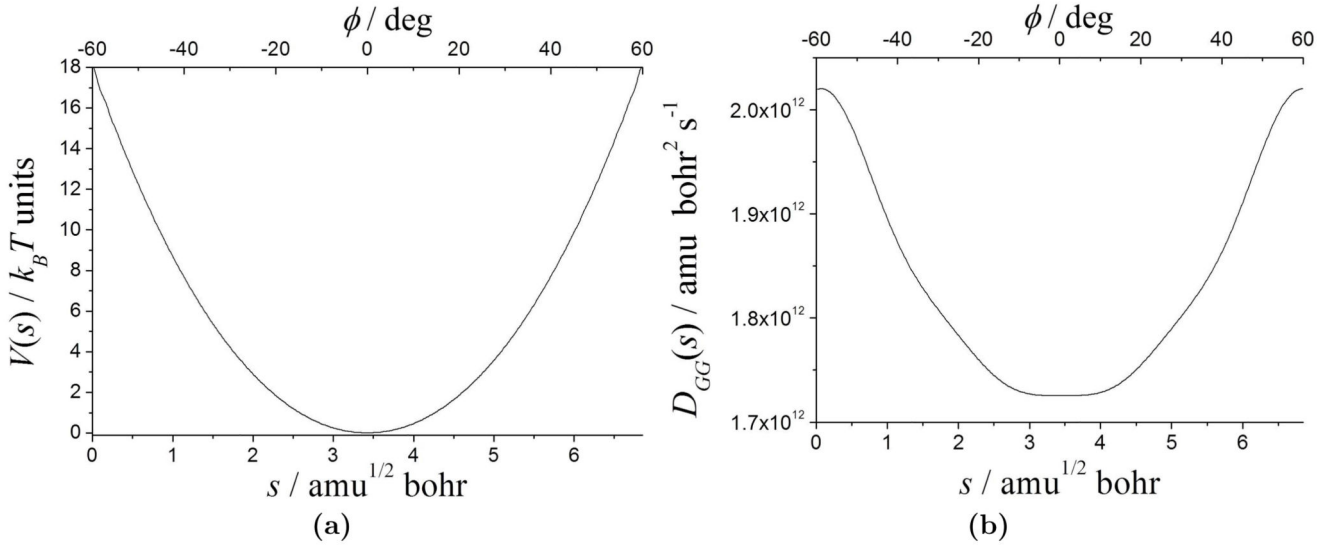

Figure 5.

Calculated potential energy of cyclopentene from the relaxed scan (panel a) and diffusion along the generalized coordinate (panel b). The upper axis shows the corresponding internal coordinate upon which the scan is performed. (T = 298.15 K)

Europe PMC Funders Author Manuscripts

Europe PMC Funders Author Manuscripts

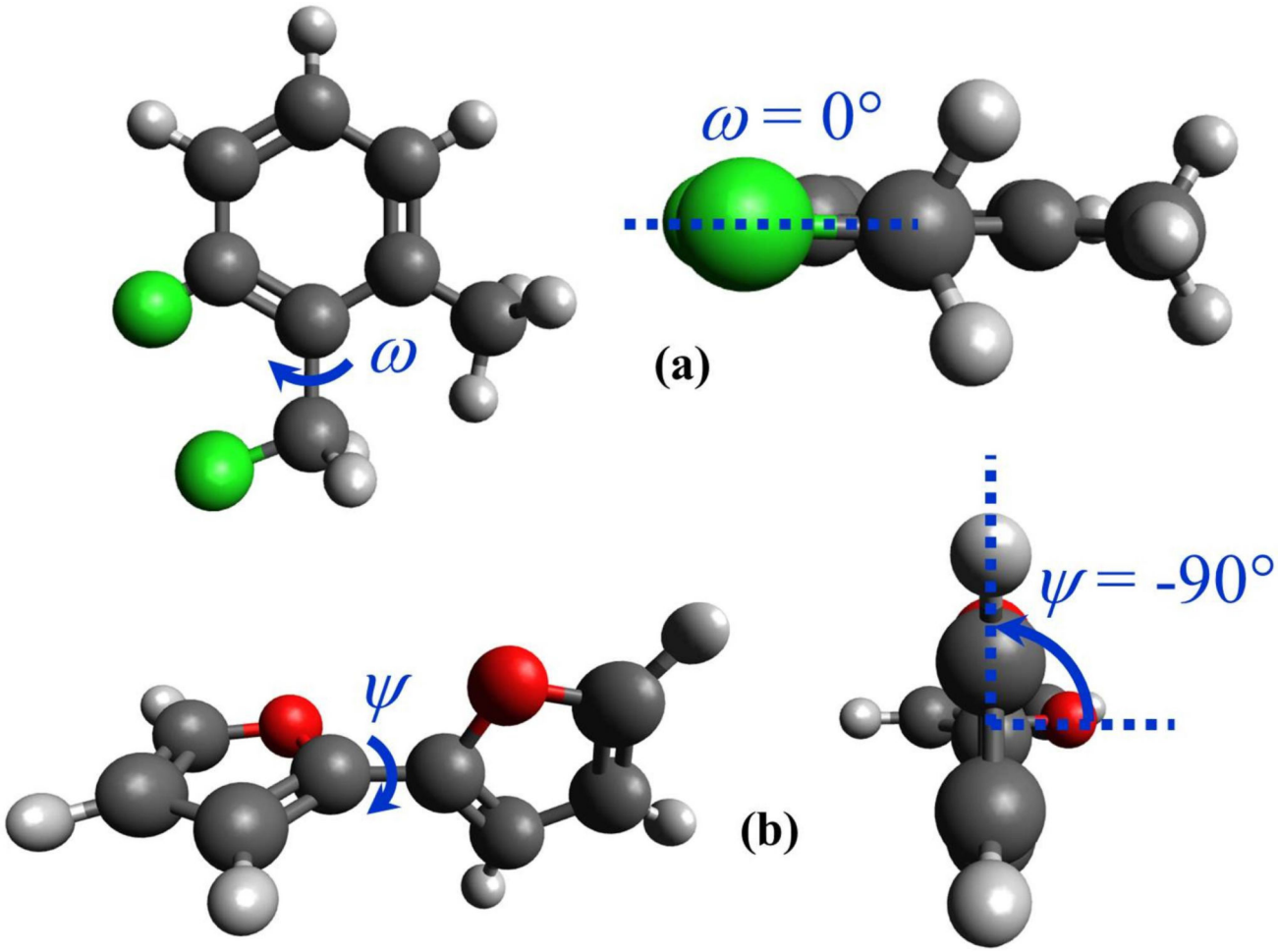

Figure 6.
Sketch of 3-chloro-2-(chloromethyl)toluene (panel a) and 2,2'-bifuran (panel b) starting conformations for the scans along the highlighted internal coordinate.

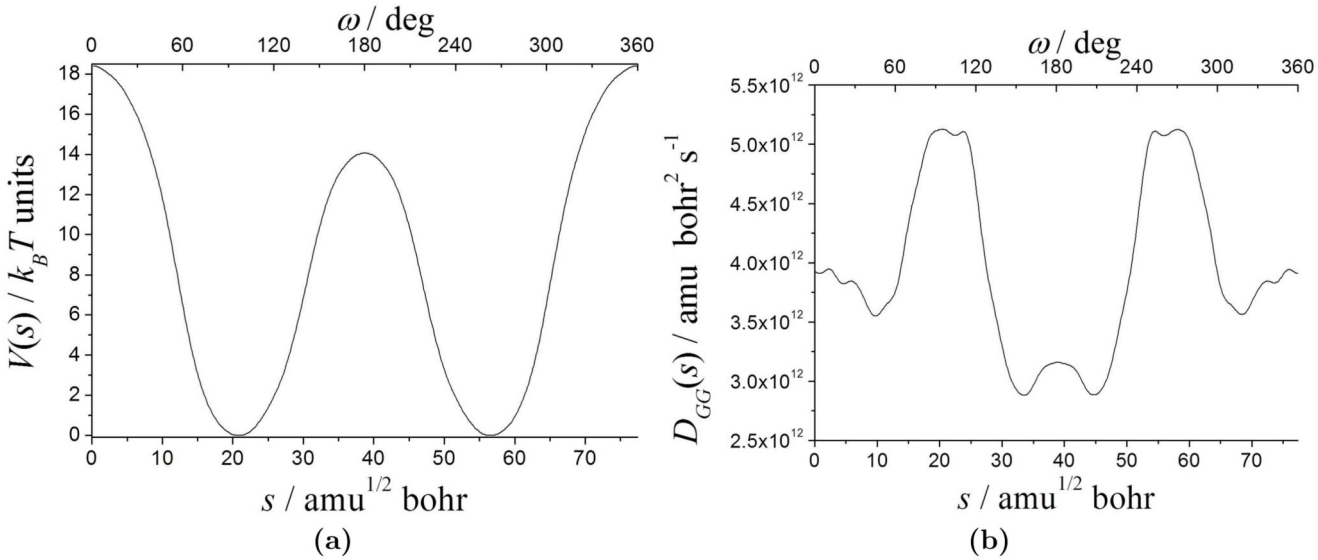

Figure 7.

Calculated potential energy of 3-chloro-2-(chloromethyl)toluene from the relaxed scan (panel a) and diffusion along the generalized coordinate (panel b). The upper axis shows the corresponding internal coordinate upon which the scan is performed. (T = 298.15 K)

Europe PMC Funders Author Manuscripts

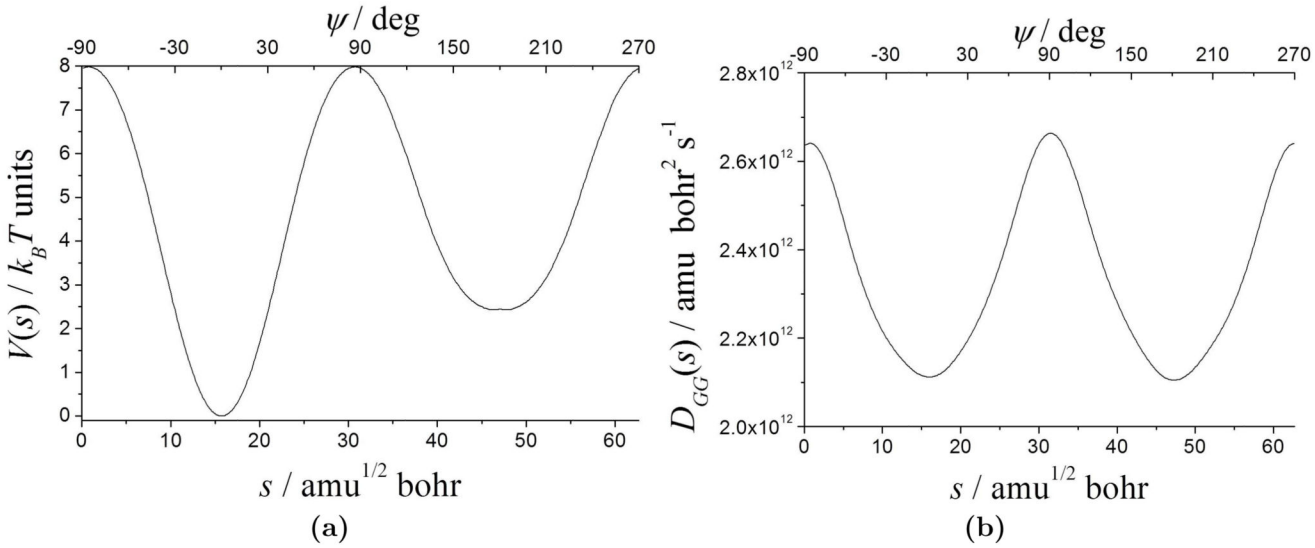

Figure 8.

Calculated potential energy of 2,2'-bifuran from the relaxed scan (panel a) and diffusion along the generalized coordinate (panel b). The upper axis shows the corresponding internal coordinate upon which the scan is performed. (T = 298.15 K)

Europe PMC Funders Author Manuscripts